


 Cite this: *RSC Adv.*, 2022, **12**, 21548

Cationic palladium(II)-catalyzed synthesis of substituted pyridines from α,β -unsaturated oxime ethers†

Takahiro Yamada, Yoshimitsu Hashimoto, Kosaku Tanaka, III, Nobuyoshi Morita and Osamu Tamura *

An efficient method for the synthesis of multi-substituted pyridines from β -aryl-substituted α,β -unsaturated oxime ethers and alkenes *via* Pd-catalyzed C–H activation has been developed. The method, using $\text{Pd}(\text{OAc})_2$ and a sterically hindered pyridine ligand, provides access to various multi-substituted pyridines with complete regioselectivity. Mechanistic studies suggest that the pyridine products are formed by Pd-catalyzed electrophilic C–H alkenylation of α,β -unsaturated oxime followed by aza-6 π -electrocyclization. The utility of this method is showcased by the synthesis of 4-aryl-substituted pyridine derivatives, which are difficult to synthesize efficiently using previously reported Rh-catalyzed strategies with alkenes.

 Received 23rd June 2022
 Accepted 14th July 2022

 DOI: 10.1039/d2ra03875g
rsc.li/rsc-advances

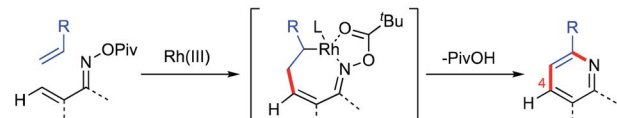
Introduction

Substituted pyridine scaffolds are ubiquitous in medicinal chemistry. A recent analysis of the ring systems in all FDA-approved pharmaceutical drugs revealed the pyridine ring to be the most prevalent nitrogen-containing heteroaromatic motif.¹ In particular, appropriately substituted pyridines exhibit a wide range of biological activities.² In this context, the development of a versatile approach to build substituted pyridines from readily accessible building blocks is a topic of continuing interest for synthetic chemists. Classical methods to access substituted pyridines generally involve either carbonyl condensation³ or [2 + 2 + 2] cycloaddition.⁴ However, these methods require harsh reaction conditions and only limited pyridine substitution patterns can be synthesized. Recently, remarkable progress has been reported, with the assembly of the pyridine core *via* [4 + 2] cycloaddition from 1-azadienes and two-carbon π -components.⁵ Rh-catalyzed [4 + 2] cycloaddition approaches are particularly useful, and can provide access to multi-substituted pyridines from α,β -unsaturated oximes with alkynes or alkenes.⁶ For example, the Rovis group reported that the Rh(III)-catalyzed coupling of α,β -unsaturated oximes with activated alkenes was a useful approach to build substituted pyridines with good regioselectivity (Scheme 1a).^{6e} Interestingly, this reaction involves a 7-membered rhodacycle intermediate, which undergoes C–N bond formation/N–O bond cleavage to

furnish the pyridine product. Unfortunately, high yields are obtained only with β -unsubstituted α,β -unsaturated oximes. Therefore, efficient strategies to construct 4-substituted pyridines from readily accessible β -substituted α,β -unsaturated oximes with high regioselectivity are still needed.

Umpolung reactivity (polarity inversion) is an effective strategy for organic synthesis, as demonstrated by the wealth of examples that have contributed to the development of synthetic chemistry.⁷ Especially, carbonyl Umpolung using oximes and hydrazones, which have an electron-donating hetero atom in an imine functionality, has been developed to invert the electrophilic reactivity of carbonyl compounds to a nucleophilic character.^{8,9} However, with regard to α,β -unsaturated oximes, there are only a few reports on extension of this electron-donating ability to conjugated olefins.¹⁰ Because of the electron-donating effect of an electron lone pair, conjugated systems of

a. Rh-catalyzed pyridine synthesis from α,β -unsaturated oxime ester with alkenes



b. Pd-catalyzed pyridine synthesis from α,β -unsaturated oxime ether with alkenes



Showa Pharmaceutical University, Machida, Tokyo 194-8543, Japan. E-mail: tamura@ac.shoyaku.ac.jp

† Electronic supplementary information (ESI) available. CCDC 2166741. For ESI and crystallographic data in CIF or other electronic format see <https://doi.org/10.1039/d2ra03875g>

Scheme 1 Synthesis of substituted pyridines from α,β -unsaturated oximes.



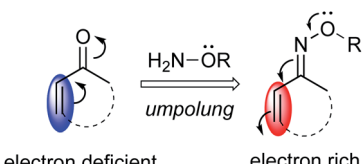


Fig. 1 Umpolung reactivity of α,β -unsaturated oximes.

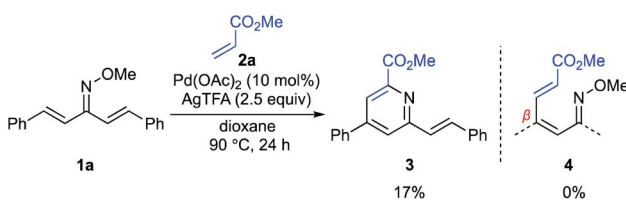
α,β -unsaturated oximes, especially at the β -position, can potentially exhibit nucleophilic reactivity (Fig. 1).

With this unique Umpolung reactivity in mind, we have developed a C–H functionalization of the β -position of α,β -unsaturated oximes using cationic Pd(II) catalysts.¹¹ In this reaction, α,β -unsaturated oximes react with highly electrophilic cationic Pd(II) species, such as $\text{Pd}(\text{OCOCF}_3)^+$, at the nucleophilic β -position *via* electrophilic C–H activation. Based on this work, we have recently communicated a new method for the synthesis of multi-substituted pyridines from α,β -unsaturated oxime ethers *via* a two-step process: cationic Pd(II)-catalyzed electrophilic C–H alkenylation of α,β -unsaturated oximes followed by aza-6 π -electrocyclization (Scheme 1b).¹² The key features of our method are its operational simplicity, broad substrate scope, and the use of a general $\text{Pd}(\text{OAc})_2$ catalyst to obtain 4-substituted pyridine derivatives with complete regioselectivity. This work complements previously reported pyridine synthetic methods, since 4-unsubstituted pyridines can already be easily prepared with alkenes by using Rh-catalyzed strategies (Scheme 1a *vs.* b). In this article, we present a full account of this work, together with additional experimental data to provide insights into the mechanism of the cationic palladium(II)-catalyzed electrophilic C–H activation of α,β -unsaturated oximes.

Results and discussion

Optimization of pyridine ligand

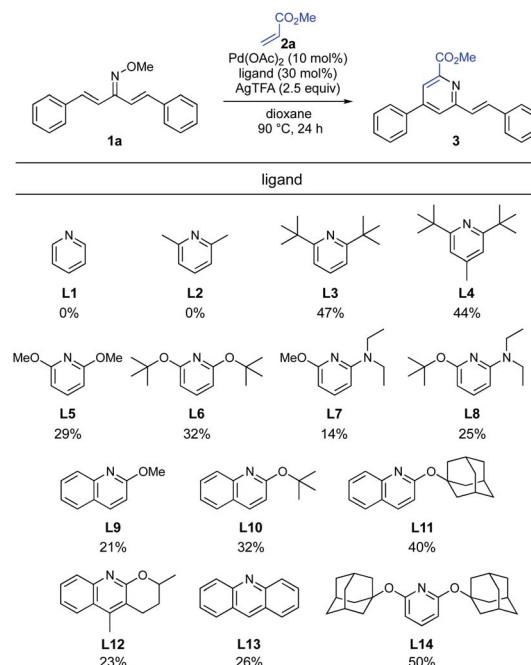
For the examination of this pyridine synthesis, we first chose a symmetrical oxime **1a** as a model substrate (Scheme 2). Based on our experience in the development of oxime chemistry,¹¹ oxime ethers of β -substituted α,β -unsaturated ketones readily undergo *E/Z* isomerism, which might interfere with optimization of the reaction. Thus, our studies began with examination of the reaction of symmetrical α,β -unsaturated *O*-methyl oxime **1a** and methyl acrylate (**2a**) in the presence of $\text{Pd}(\text{OAc})_2$ as a catalyst (Scheme 2). With silver trifluoroacetate (AgTFA) as an oxidant and dioxane as a solvent, the desired pyridine **3** was obtained in 17% yield. It should be noted here that no β -



Scheme 2 Initial experiment.

alkenylation product **4** was observed, suggesting that aza-6 π -electrocyclization of **4** and subsequent aromatization proceed rapidly to furnish the pyridine **3**. Although other solvents such as toluene, 1,2-dichloroethane, DMF, and HFIP were examined, the product yield was not improved. Unfortunately, the high temperature (over 100 °C) reaction caused substrate decomposition.

Our experience in the development of Pd-catalyzed β -selective C–H functionalization of α,β -unsaturated oximes showed that the identification of a suitable catalyst ligand would be the key to establish the optimal protocol.¹¹ Recently, Ji and co-workers have reported that the addition of pyridine promoted the Pd-catalyzed C(sp²)-H alkenylation of *O*-methyl ketoximes.¹³ With Ji's results in mind, we explored the effect of pyridine derivatives as ligands (Scheme 3). Although the addition of pyridine (**L1**) and 2,6-lutidine (**L2**) unexpectedly inhibited the reaction, sterically hindered 2,6-di-*tert*-butyl pyridine (**L3**) and 2,6-di-*tert*-butyl 4-methyl pyridine (**L4**) significantly increased the reactivity and the desired pyridine **3** was obtained in 47% and 44% yields, respectively. The use of 2,6-dialkoxypyridines **L5** and **L6**, which are more electron-rich ligands than pyridine (**L1**), afforded the pyridine **3** in 29% and 32% yields, respectively. Unfortunately, the reactions employing pyridines **L7** and **L8**, containing a stronger electron-donating dialkylamino group, decreased the product yield. This was presumably because pyridine with a strong coordination ability deactivates the Pd catalyst. Next, we tested a series of 2-alkoxylquinoline derivatives (**L9**–**L12**). Despite the ineffectiveness of 2-methoxyquinoline (**L9**), the product yield was improved when a quinoline ligand bearing a bulkier side chain, such as *tert*-butoxy



Scheme 3 Optimization of pyridine ligand. ^aReaction conditions: **1a** (0.2 mmol, 1.0 equiv.), **2a** (3.0 equiv.), $\text{Pd}(\text{OAc})_2$ (10 mol%), ligand (30 mol%), AgTFA (2.5 equiv.), dioxane (2.0 mL), 90 °C, 24 h. Isolated yield.

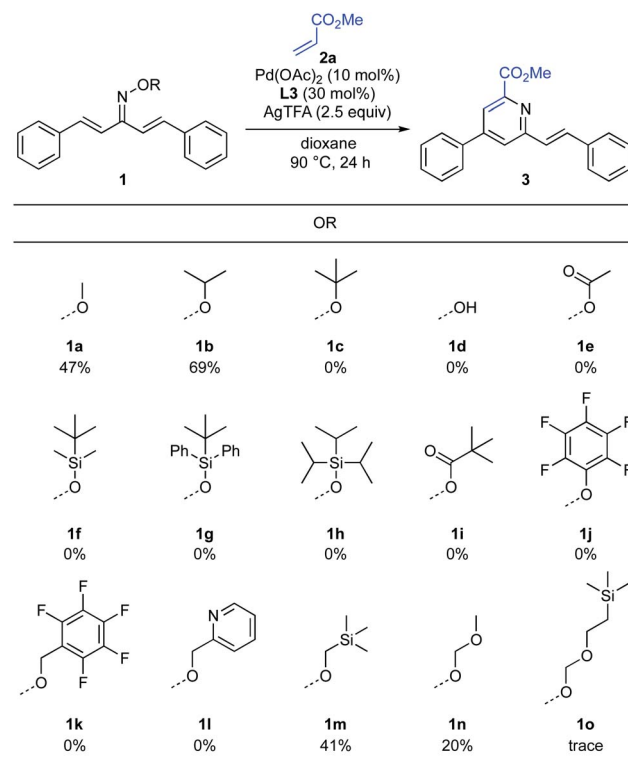
(**L10**) or 1-adamantyloxy (**L11**), was used. This substituent effect suggested that the steric hindrance around the nitrogen atom of the quinoline ligand is crucial for high reactivity. Unexpectedly, tricyclic quinoline-derived ligand **L12**, developed by Yu and co-workers,¹⁴ and acridine (**L13**) led to loss of reactivity. Anticipating a positive effect of a bulkier ligand, we prepared 2,6-diadamantyloxy pyridine (**L14**) in one step from 2,6-difluoropyridine and 1-adamantanol. To our delight, the use of **L14** improved the reactivity and afforded **3** in 50% yield.

Effect of Pd catalyst and oxidant

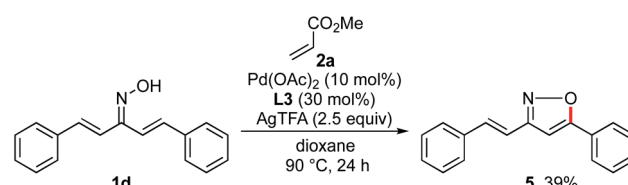
Next, the effects of palladium catalyst and oxidizing agent were investigated (Table 1). Without AgTFA, the desired product **3** was not formed (entry 2). When we employed PdCl₂ instead of Pd(OAc)₂, the reaction proceeded, albeit at the expense of a significantly decreased yield (entry 3). The use of Pd(TFA)₂ slightly increased the reactivity and afforded **3** in 53% yield (entry 4). When AgOAc was used as an oxidant, the reaction efficiency was significantly decreased, indicating that the addition of AgTFA is necessary for the C–H alkenylation reaction to proceed (entry 5). These results are consistent with the hypothesis that Pd(OCOCF₃)⁺ generated *in situ* from Pd(OAc)₂ and AgTFA is the reactive species in this transformation (Scheme 1b).¹⁵

Optimization of oxime ether and its influence on reactivity

To improve the reaction efficiency, we next focused on modification of the oxime ether moiety (Scheme 4). Tuning the structure of the oxime ether moiety makes it possible to change the electronic state and nucleophilic reactivity of α,β -unsaturated oxime.¹¹ Among the oxime ethers surveyed, *O*-isopropyl oxime **1b** improved the reactivity and the product yield increased to 69%. In the case of the highly sterically hindered *O*-*tert*-butyl oxime **1c**, the starting material was completely recovered. The parent oxime **1d** afforded none of the desired pyridine, instead undergoing intramolecular cyclization to give isoxazole **5** in 39% yield (Scheme 5). Isoxazole **5** was similarly



Scheme 4 Optimization of oxime ether. ^aReaction conditions: **1** (0.2 mmol, 1.0 equiv.), **2a** (3.0 equiv.), Pd(OAc)₂ (10 mol%), **L3** (30 mol%), AgTFA (2.5 equiv.), dioxane (2.0 mL), 90 °C, 24 h. Isolated yield.



Scheme 5 Formation of isoxazole **5**.

Table 1 Effect of Pd catalyst and oxidant^a

Entry	Pd cat.	Oxidant	Yield
1	Pd(OAc) ₂	AgTFA	47%
2	Pd(OAc) ₂	None	0%
3	PdCl ₂	AgTFA	10%
4	Pd(TFA) ₂	AgTFA	53%
5	Pd(TFA) ₂	AgOAc	Trace

^a Reaction conditions: **1a** (0.2 mmol, 1.0 equiv.), **2a** (3.0 equiv.), Pd cat. (10 mol%), **L3** (30 mol%), oxidant (2.5 equiv.), dioxane (2.0 mL), 90 °C, 24 h. Isolated yield.

observed with the *O*-acetyl oxime **1e** and *O*-silyl oximes (**1f–1h**). Formation of **5** may proceed *via* deprotection of oxime ester **1e** or silyl oximes (**1f–1h**) to release the parent oxime **1d**, followed by intramolecular cyclization.¹⁶ Although various oximes bearing *O*-pivaloyl (**1i**), *O*-pentafluorophenyl (**1j**), *O*-pentafluorobenzyl (**1k**), and *O*-pyridylmethyl (**1l**) groups were examined, none of them underwent pyridine formation. Heteroatom-containing alkyl oxime ethers such as *O*-methyl trimethylsilyl oxime **1m**, *O*-methoxymethyl oxime **1n**, or *O*-SEM oxime **1o** afforded the desired pyridine, but the product yield was significantly decreased.

With the optimal oxime ether moiety (isopropyl) in hand, the reaction conditions were further screened (Table 2). Introduction of ligand **L14** in place of **L3** improved the yield from 69% to 76% (entry 2). After a brief investigation of the amount of oxidant, we found the use of 5.0 equiv. of AgTFA to be optimal, providing the pyridine **3** in 85% yield (entries 3 and 4).



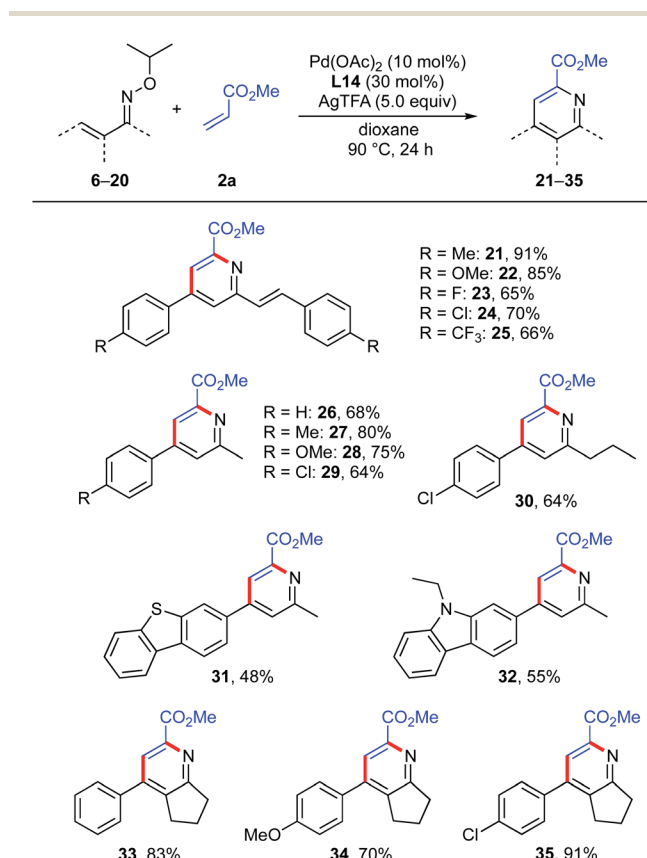
Table 2 Optimization of the reaction conditions^a

Entry	Ligand	AgTFA (x equiv.)	Yield	
			Yield	Yield
1	L3	2.5	69%	
2	L14	2.5	76%	
3	L14	4.0	77%	
4	L14	5.0	85%	

^a Reaction conditions: **1b** (0.2 mmol, 1.0 equiv.), **2a** (3.0 equiv.), Pd(OAc)₂ (10 mol%), ligand (30 mol%), AgTFA (x equiv.), dioxane (2.0 mL), 90 °C, 24 h. Isolated yield.

Substrate scope

With the optimal oxime moiety and reaction conditions in hand, we surveyed the generality of this multi-substituted pyridine synthesis by examining the reaction of various α,β -unsaturated oximes with methyl acrylate (Scheme 6).

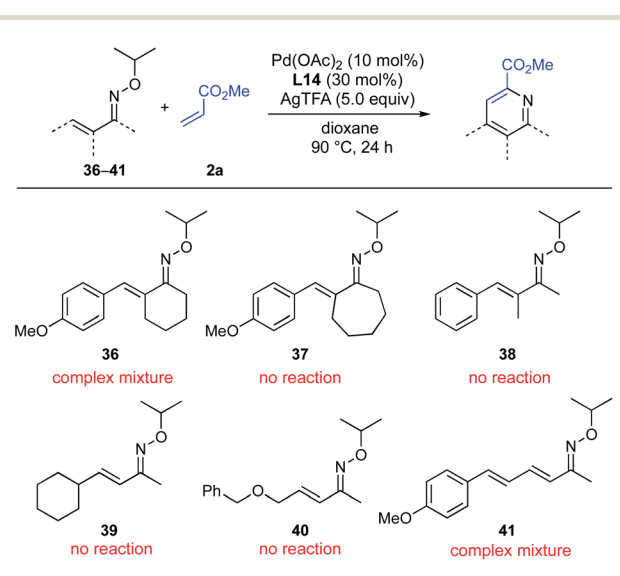


Scheme 6 Scope of α,β -unsaturated oxime ethers. ^aReaction conditions: **1** (0.2 mmol, 1.0 equiv.), **2a** (3.0 equiv.), Pd(OAc)₂ (10 mol%), **L14** (30 mol%), AgTFA (5.0 equiv.), dioxane (2.0 mL), 90 °C, 24 h. Isolated yield.

Symmetrical oximes bearing an electron-donating group (Me, OMe), halogens (F, Cl) and an electron-withdrawing CF₃ group at the *para*-position of the phenyl ring afforded the expected 2-allyl pyridines (**21-25**) in good yields (65–91%). Notably, unsymmetrical ketoximes were tolerated, affording the corresponding pyridines (**26-30**) in good yields (64–80%). Oximes with heteroaromatics such as dibenzothiophene and carbazole were also acceptable, and furnished the desired pyridines **31** and **32** in 48% and 55% yields, respectively. This reaction also worked well with cyclized oximes derived from benzylidene cyclopentanone derivatives, giving the desired 2,3,4,6-tetrasubstituted pyridines (**33-35**) in good yields.

Although the 5-membered cyclized oximes (**18-20**), giving pyridines **33-35**, were found to be suitable substrates for this pyridine synthesis, oximes with 6-membered (**36**) and 7-membered ring (**37**) were not tolerated, resulting only in complex mixtures or no reaction (Scheme 7). With α -methyl-substituted acyclic oxime **38**, the reaction did not proceed at all and the raw material was completely recovered. Unfortunately, neither a β -alkyl substituent (**39** and **40**) nor a β -allyl substituent (**41**) was tolerated, indicating that the substrate scope of this reaction is limited to β -aryl-substituted α,β -unsaturated oximes.

The high reactivities of 2-benzylidene cyclopentenone oximes (**18-20**) probably originate from the planarity of the conjugated system arising from the 5-membered ring structure, which enables efficient conjugation from oxime–oxygen to carbon–carbon double bond, imparting electron-donating character. As shown in Fig. 2, X-ray crystallographic analysis of α,β -unsaturated oxime **18** confirmed that the conjugated system of **18** is almost planar and the dihedral angle (N=C–C=C) is 6°.¹⁶ On the other hand, computational studies with density functional theory (DFT)^{17,18} revealed that the conjugated systems of 6-membered and 7-membered α,β -unsaturated oximes **36** and **37** are quasi-planar, and the dihedral angles are 31° and 52°, respectively. These results clearly indicate that highly planar



Scheme 7 Unsuccessful substrates.



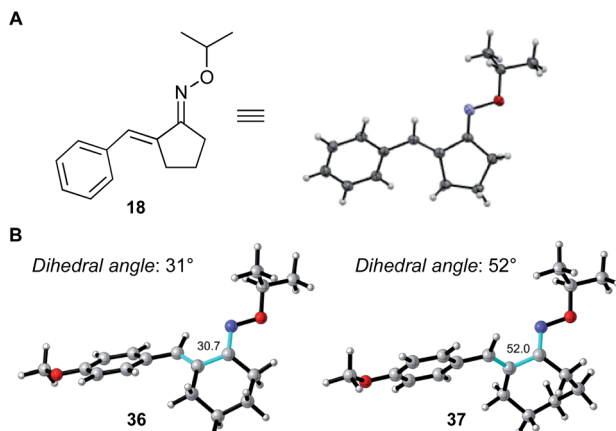
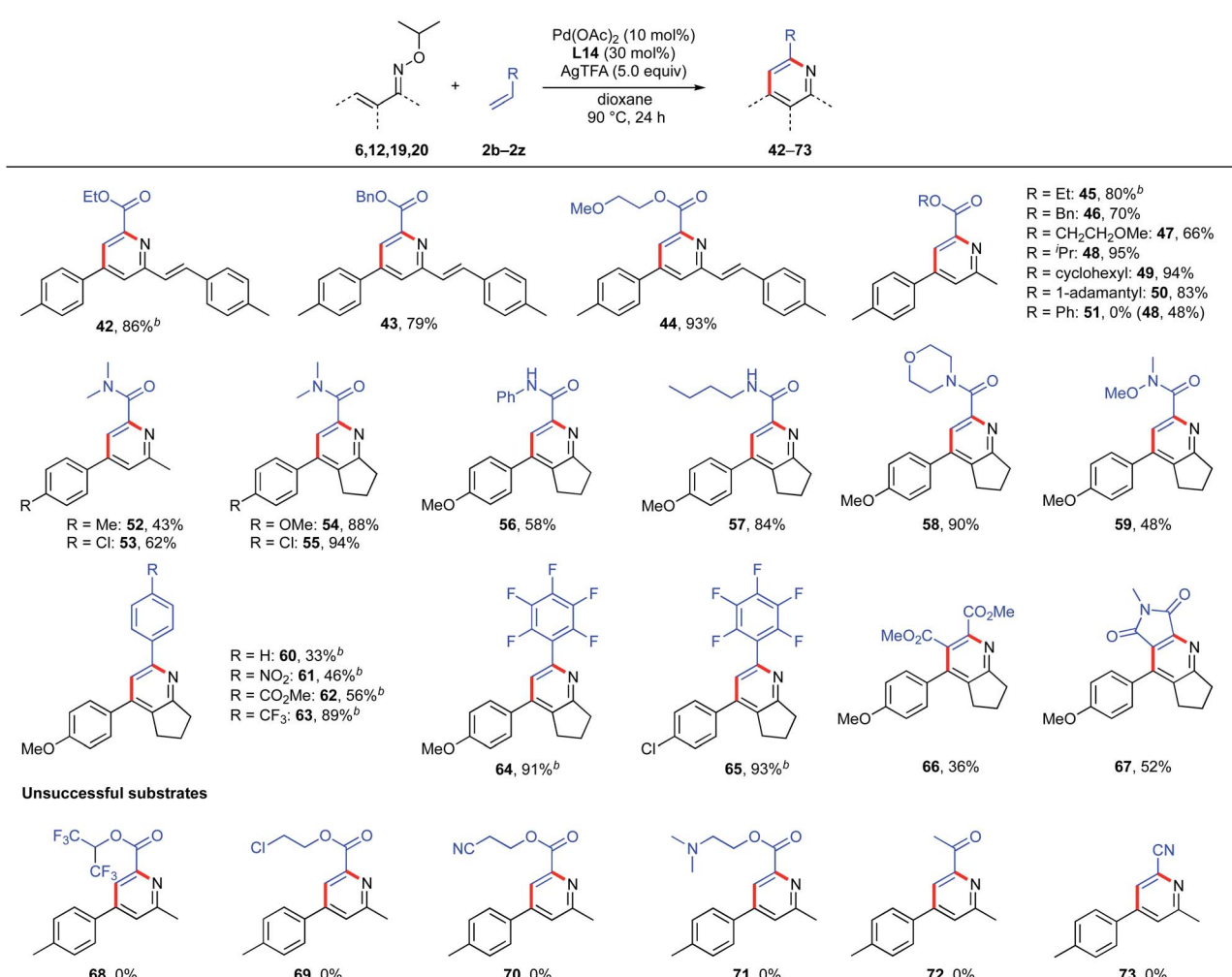


Fig. 2 (A) ORTEP representation of oxime 18. (B) Calculated structures and $N=C-C=C$ dihedral angle (highlighted in light green) of oximes 36 and 37.¹⁸

conformation of α,β -unsaturated oxime is favorable for the progress of this Pd-catalyzed C–H activation reaction. This also explains the lack of reactivity of 38.

Next, we examined the scope with respect to the partner olefins (Scheme 8). Acrylates bearing ethyl, benzyl, and methoxy ethyl substituents were found to react smoothly, giving the expected 2-phenylethenyl pyridines (42–44) in 86%, 79%, and 93% yields, respectively. Unsymmetrical ketoximes with various acrylates were also compatible and the corresponding pyridines (45–47) were obtained in good yields. Notably, acrylates bearing sterically bulky alkyl groups, such as isopropyl, cyclohexyl, and 1-adamantyl groups worked well, affording the desired products (48–50) in excellent yields. Unexpectedly, the use of phenyl acrylate as a partner olefin gave not pyridine 51 but pyridine, with isopropyl ester 48 as the major product. This product was probably formed by ester exchange reaction between the corresponding pyridine 51 and *in situ*-generated isopropanol (see below, Mechanistic studies section, Scheme 10). Other acrylate derivatives such as acrylamides were also tolerated and provided the corresponding pyridines 52 and 53 in moderate yields. To our surprise, 5-membered cyclized oximes (19 and 20) reacted efficiently with *N,N*-dimethyl acrylamide, giving the desired tetra-substituted pyridines 54 and 55 in excellent yields.



Scheme 8 Scope of olefins. ^aReaction conditions: oxime (0.1–0.2 mmol, 1.0 equiv.), alkene (1.5 equiv.), Pd(OAc)_2 (10 mol%), L14 (30 mol%), AgTFA (5.0 equiv.), dioxane (2.0 mL), 90°C , 24 h. Isolated yield. ^b3.0 equiv. of alkene was used.



To demonstrate the generality and utility of this multi-substituted pyridine synthesis, the reactions of 5-membered cyclized oximes with other unsaturated olefins were also tested. Various acrylamide derivatives such as phenyl acrylamide, *n*-butyl acrylamide, and 4-acryloylmorpholine were found to be suitable coupling partners, giving the desired products (56–58) in 58%, 84% and 90% yields, respectively. Weinreb amide-derived acrylamide was also tolerated, giving the corresponding pyridine 59 in moderate yield. Various styrene derivatives containing electron-withdrawing groups such as nitro and ester were also tolerated and afforded the expected pyridines (60–62) in moderate yields. Notably, 4-trifluoromethyl styrene and pentafluorostyrene reacted smoothly with cyclized oximes, providing the corresponding pyridines 63, 64 and 65 in excellent yields. Furthermore, this pyridine synthesis is effective not only for mono-substituted olefins, but also for di-substituted olefins. With dimethyl maleate and *N*-methyl maleimide, the corresponding penta-substituted pyridines 66 and 67 were obtained in 36% and 52% yields, respectively. Unfortunately, acrylates bearing hexafluoroisopropyl, 2-chloroethyl, 2-cyanoethyl, and 2-dimethylaminoethyl substituents were not tolerated (68–71). With methyl vinyl ketone or acrylonitrile, the reaction did not proceed at all (72 and 73) and the starting material was recovered.

Effect of catalyst loading and the amount of AgTFA

Next, the effect of catalyst loading on the product yield was investigated (Table 3). With decreasing amounts of $\text{Pd}(\text{OAc})_2$ to 1 mol% and **L14** to 3 mol%, the reaction was clearly slowed down. However, when the reaction time was extended to 80 h, the desired pyridine **74** was obtained in 77% yield (entry 2). Next, the effect of the amount of AgTFA on the product yield was investigated. The use of 1.2 and 2.5 equiv. of AgTFA led to loss of reactivity, and the product yields were decreased to 27% and 44% yields, respectively (entries 3 and 4). However, the use of 10

equiv. of AgTFA improved the reactivity and afforded pyridine **74** in 91% yield (entry 5). These results indicated that the amount of AgTFA is of critical importance to the reaction efficiency.

Mechanistic studies

(i) Control experiments with specific substrates and conditions. To gain insight into the reaction mechanism, some competitive reactions were conducted (Table 4). Competitive reaction of methyl acrylate (**2a**) with α,β -unsaturated oximes, bearing a methyl and a chloro group at the *para*-position of the phenyl ring, gave the corresponding pyridines in 53% and 27% yields, respectively (entry 1). Similarly, the reactivities of compounds with other substituents (OMe, Me, H, and Cl) were investigated (entries 2–4). The relative reactivity was found to be in order of OMe > Me > H > Cl-substituted α,β -unsaturated oximes, indicating that the reaction could proceed in an electrophilic manner. The results of these competitive experiments were consistent with a mechanism that involves a cationic $\text{Pd}(\text{II})$ -catalyzed electrophilic C–H activation¹⁵ rather than a standard concerted metalation–deprotonation (CMD) mechanism.¹⁹

The structure of the oxime ether moiety clearly affected the reactivity, and the *O*-isopropyl oxime was found to be optimal (Scheme 4). The increased reactivity of *O*-isopropyl oxime compared to other oxime ethers may be due to the dual role in the C–H alkenylation reaction: (1) the more nucleophilic character of α,β -unsaturated *O*-isopropyl oxime arising from the strong electron-donating effect of the isopropoxy group in the imino functionality promotes the electrophilic C–H activation step; (2) *in situ*-generated 2-propanol, which is generated in the pyridine ring formation step, may have a less adverse effect on the catalytic reactivity. Indeed, with oxime **18** and pentafluorostyrene (**2r**) as model substrates, the addition of a stoichiometric amount of either methanol or isopropanol to the reaction mixture under standard reaction conditions had a detrimental effect on the reaction efficiency, and the product yields dropped from 83% to 54%, and 66%, respectively (Table 5).²⁰ This result indicates that the *in situ*-generated alcohol decreases the reaction efficiency, presumably due to deactivation of the Pd catalyst. It should also be noted here that the product yield with the addition of isopropanol was better than that with methanol (entry 2 vs. 3).

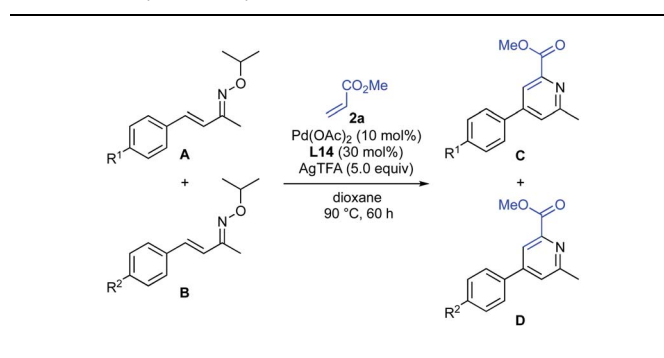
(ii) Deuterium labelling experiments. To probe the nature of this C–H activation reaction, we performed isotope labelling experiments (Scheme 9a). Treatment of α,β -unsaturated oxime **18** with excess amount of acetic acid-*d*₄ in the presence of $\text{Pd}(\text{OAc})_2$, **L14**, and AgTFA resulted in significant deuterium incorporation at the β -position of oxime **18** (Scheme 9, eqn (1)). This result implies that the Pd–C bond formation is reversible. In the same reaction, nearly complete deuterium incorporation at the α -methylene group of oxime **18** occurred, indicating reversible deprotonation at this position under these reaction conditions. In general, deuteration at the α -position of oximes likely takes place with imine–enamine tautomerization. Interestingly, in the absence of catalysts and AgTFA, very little

Table 3 Effect of catalyst loading and the amount of AgTFA^a

Entry	$\text{Pd}(\text{OAc})_2$ (x mol%)	L14 (y mol%)	AgTFA (z equiv.)	Time	Yield			
						18	2r	74
1	10	30	5.0	24 h	83%			
2	1	3	5.0	80 h	77%			
3	10	30	1.2	24 h	27%			
4	10	30	2.5	24 h	44%			
5	10	30	10	24 h	91%			

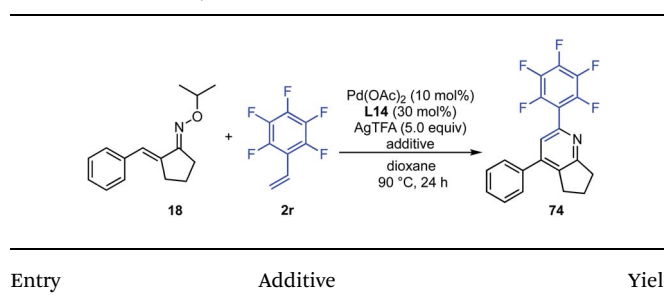
^a Reaction conditions: **18** (0.2 mmol, 1.0 equiv.), **2r** (3.0 equiv.), $\text{Pd}(\text{OAc})_2$ (x mol%), **L14** (y mol%), AgTFA (z equiv.), dioxane (2.0 mL), 90 °C, 24 h. Isolated yield.



Table 4 Competitive experiments^a

Entry	Substrates		Product yield		
	R ¹ (A, C)	R ² (B, D)	C	D	C/D
1	Me	Cl	53%	27%	1.9
2	OMe	Me	52%	29%	1.8
3	Me	H	75%	44%	1.7
4	H	Cl	34%	26%	1.3

^a Reactions were conducted with 0.2 mmol of oxime A and 0.2 mmol of oxime B. Product yield and the ratio of C and D (C/D) were determined by ¹H NMR analysis of the isolated products.

Table 5 Control experiments^a

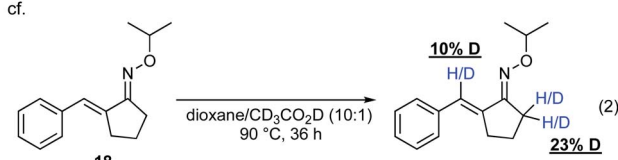
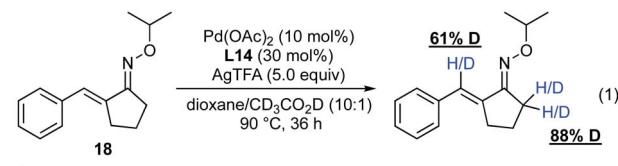
Entry	Additive	Yield
1	None	83%
2	MeOH (1.0 equiv.)	54%
3	ⁱ PrOH (1.0 equiv.)	66%

^a Reaction conditions: **18** (0.2 mmol, 1.0 equiv.), **2r** (3.0 equiv.), Pd(OAc)₂ (10 mol%), **L14** (30 mol%), AgTFA (5.0 equiv.), additive (1.0 equiv.), dioxane (2.0 mL), 90 °C, 24 h. Isolated yield.

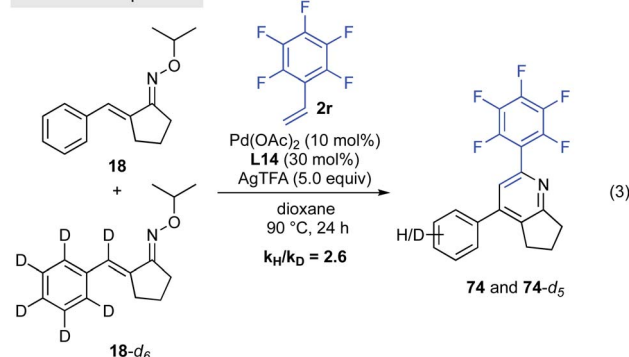
deuterium incorporation at the corresponding sites in oxime **18** was observed (Scheme 9, eqn (2)). A kinetic isotope effect study provided further insight regarding this C–H activation mechanism. A significant isotope effect was observed ($k_H/k_D = 2.6/1$), indicating that the C–H activation at the β -position of the α , β -unsaturated oxime could be the rate-limiting step, although further kinetic studies might be needed to confirm this (Scheme 9, eqn (3)).

(iii) **Mechanistic studies on pyridine ring formation.** Next, we carried out mechanistic studies on pyridine ring formation. The formation of pyridines from α , β -unsaturated oximes would involve aza-6 π -electrocyclization. Thus, Pd-catalyzed electrophilic C–H alkenylation of α , β -unsaturated oxime generates the

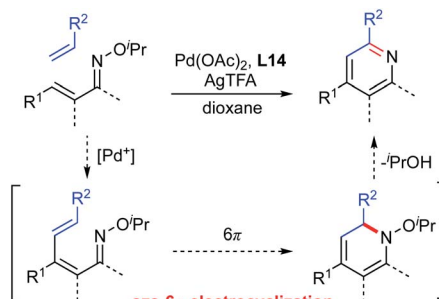
a. Deuterium labelling experiments



b. Kinetic isotope effect



Scheme 9 Deuterium labelling experiments.

Scheme 10 Pyridine formation via aza-6 π -electrocyclization.

1-azatriene intermediate, which undergoes electrocyclization and aromatization with release of isopropanol to furnish the pyridine product (Scheme 10). Such aza-6 π -electrocyclization has been demonstrated with various substrates, including oxime ethers.²¹ However, the expected 1-azatriene intermediate could not be detected in our study, probably because 6 π -electrocyclization of the azatriene proceeds very rapidly.

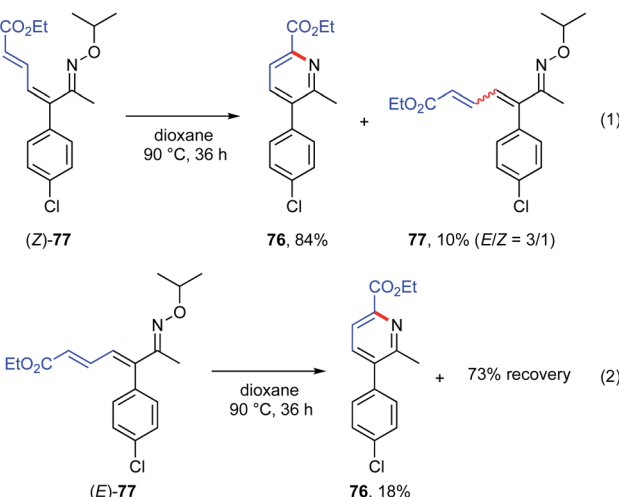
To gain insight into the mechanism of pyridine ring formation, additional experiments were conducted (Table 6). When the reaction was performed with β -unsubstituted oxime **75** and ethyl acrylate (**2b**) under the same reaction conditions for 4 h, 1-azatriene **77** was obtained in 36% yield as a 1.3 : 1 mixture of *E/Z* isomers, but the expected pyridine **76** was not detected (entry 1). However, when the reaction time was extended to 36 h, the pyridine **76** was obtained in 28% yield along with 1-azatriene **77** in 11% yield (entry 2). It should be



Table 6 Reaction of β -unsubstituted α,β -unsaturated oxime with alkene^a

Entry	Time	76	77
1	4 h	0%	36% (<i>E/Z</i> = 1.3/1)
2	36 h	28%	11% (<i>E</i> -isomer only)

^a Conditions: see Scheme 6. Isolated yield. The wavy bond of 1-azatriene 77 indicates a mixture of *cis* and *trans* configurations of C3–C4 olefins.



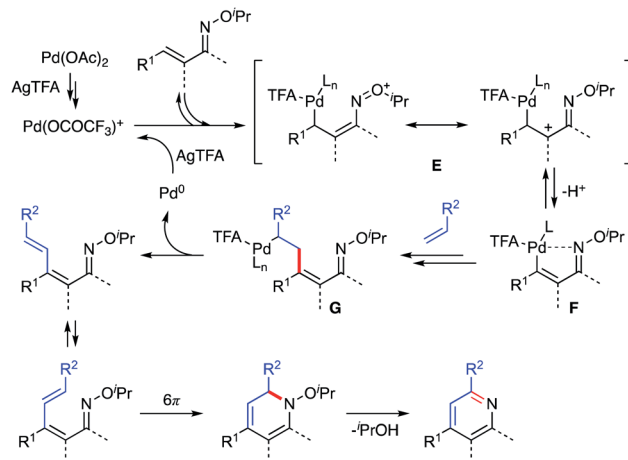
Scheme 11 Pyridine formation from 1-azatriene via aza-6 π -electrocyclization.

noted that only (*E*)-77 was recovered, suggesting that (*Z*)-77 undergoes much faster electrocyclization than (*E*)-77.

To confirm this, (*Z*)-77 was stirred in dioxane at 90 °C for 36 h. As expected, the corresponding pyridine 76 was obtained in 84% yield and a small amount of *E/Z* mixture of 77 was recovered (Scheme 11, eqn (1)). In contrast, similar treatment of (*E*)-77 gave 76 in only 18% yield and most of the (*E*)-77 was recovered (Scheme 11, eqn (2)). These results clearly indicate that the pyridine product was formed from 1-azatriene intermediates via aza-6 π -electrocyclization. Considering both recovery of *E/Z* mixture of 77 from (*Z*)-77 (eqn (1)) and formation of a small amount of 76 from (*E*)-77 (eqn (2)), *E/Z* isomerization of 1-azatriene appears to proceed to some extent under these reaction conditions.

Proposed mechanism

Based on the observations described above, a plausible reaction mechanism is shown in Scheme 12. First, $\text{Pd}(\text{OCOCF}_3)^+$ species at the β -position to generate resonance-stabilized cationic intermediate E, which kinetically releases the β -proton to give vinyl palladium F. The results of the competitive experiments are consistent with this process of electrophilic metalation followed by deprotonation. Moreover, the deuterium labelling experiments indicate that the electrophilic C–H activation process could be reversible. The subsequent Heck-type reaction of complex F with a partner alkene provides intermediate G, which undergoes β -hydride elimination and reductive elimination to afford the 1-azatriene with liberation of $\text{Pd}(0)$. The formed $\text{Pd}(0)$ can be reoxidized to $\text{Pd}(\text{OCOCF}_3)^+$ by AgTFA to complete the catalytic cycle. The resulting 1-azatriene is immediately converted to a pyridine product via aza-6 π -electrocyclization followed by aromatization. An excess amount of AgTFA would promote the formation of the cationic $\text{Pd}(\text{OCOCF}_3)^+$ species.



Scheme 12 Plausible reaction mechanism.

formed by the reaction of $\text{Pd}(\text{OAc})_2$ and AgTFA .¹⁵ Then, the α,β -unsaturated oxime reacts with the electropositive $\text{Pd}(\text{OCOCF}_3)^+$ species at the β -position to generate resonance-stabilized cationic intermediate E, which kinetically releases the β -proton to give vinyl palladium F. The results of the competitive experiments are consistent with this process of electrophilic metalation followed by deprotonation. Moreover, the deuterium labelling experiments indicate that the electrophilic C–H activation process could be reversible. The subsequent Heck-type reaction of complex F with a partner alkene provides intermediate G, which undergoes β -hydride elimination and reductive elimination to afford the 1-azatriene with liberation of $\text{Pd}(0)$. The formed $\text{Pd}(0)$ can be reoxidized to $\text{Pd}(\text{OCOCF}_3)^+$ by AgTFA to complete the catalytic cycle. The resulting 1-azatriene is immediately converted to a pyridine product via aza-6 π -electrocyclization followed by aromatization. An excess amount of AgTFA would promote the formation of the cationic $\text{Pd}(\text{OCOCF}_3)^+$ species.

Conclusion

We have developed a highly efficient and regioselective synthesis of 4-aryl substituted pyridines from β -aryl-substituted α,β -unsaturated oxime ethers. In the course of reaction optimization, we found that the catalyst ligand significantly affected the reactivity, with a sterically hindered pyridine ligand being optimal. The key features of our approach are broad substrate scope, complete regioselectivity, and high efficiency in producing 4-aryl-substituted pyridines. Mechanistic studies indicated that the $\text{Pd}(\text{II})$ -catalyzed C–H activation proceeded in an electrophilic manner, and the pyridine formation proceeded via aza-6 π -electrocyclization of β -alkenylated α,β -unsaturated oximes followed by aromatization. Considering the inherent difficulties associated with the synthesis of 4-aryl-substituted pyridines using previously developed Rh-catalyzed approaches with alkenes, we believe this transformation will be useful to enable medicinal chemists to incorporate highly complex pyridines efficiently into bioactive molecules.



Experimental section

General procedure for the synthesis of substituted pyridine derivatives

To a solution of α,β -unsaturated oxime (0.2 mmol, 1.0 equiv.), alkene (0.6 mmol, 3.0 equiv.), AgTFA (1.0 mmol, 5.0 equiv.), and **L14** (0.06 mmol, 30 mol%) in dioxane (2.0 mL) was added Pd(OAc)₂ (0.02 mmol, 10 mol%). The reaction mixture was stirred at 90 °C (silicone oil bath) for 24 h, then diluted with AcOEt and filtered through a Celite® pad (rinsed with AcOEt). The filtrate was concentrated *in vacuo*, and the crude product was purified by flash column chromatography on NH₂ silica gel to afford the pure product.

Procedure for the synthesis of pyridine 74

To a solution of α,β -unsaturated oxime **18** (46 mg, 0.2 mmol, 1.0 equiv.), pentafluorostyrene (**2r**, 116 mg, 0.6 mmol, 3.0 equiv.), AgTFA (221 mg, 1.0 mmol, 5.0 equiv.), and **L14** (22 mg, 0.06 mmol, 30 mol%) in dioxane (2.0 mL) was added Pd(OAc)₂ (4.5 mg, 0.02 mmol, 10 mol%). The reaction mixture was stirred at 90 °C (silicone oil bath) for 24 h, then diluted with AcOEt and filtered through a Celite® pad (rinsed with AcOEt). The filtrate was concentrated *in vacuo*, and the crude product was purified by flash column chromatography on NH₂ silica gel (hexane : AcOEt = 3 : 1) to afford the desired pyridine **74** (60 mg, 83% yield) as a white solid. mp 102–103 °C; IR (KBr) 1522, 1501, 1219, 990, 772 cm⁻¹; ¹H NMR (CDCl₃, 300 MHz) δ 7.60–7.30 (m, 5H), 7.26 (s, 1H), 3.25–3.09 (m, 4H), 2.30–2.15 (m, 2H). ¹³C{¹H} NMR (CDCl₃, 75 MHz) δ 167.4, 146.3 (m), 146.0, 144.7, 143.0 (m), 139.4 (m), 138.0, 136.1 (m), 135.3, 128.7, 128.6, 128.2, 123.0, 115.8 (m), 34.6, 30.8, 23.4; HRMS (EI-quadrupole) *m/z* [M]⁺ calcd for C₂₀H₁₂F₅N, 361.0890; found, 361.0888.

Conflicts of interest

There are no conflicts to declare.

Notes and references

- For selected reviews, see: (a) E. Vitaku, D. T. Smith and J. T. Njardarson, *J. Med. Chem.*, 2014, **57**, 10257–10274; (b) R. D. Taylor, M. MacCoss and A. D. G. Lawson, *J. Med. Chem.*, 2014, **57**, 5845–5859.
- For recent examples, see: (a) J. J. Cui, M. Tran-Dubé, H. Shen, M. Nambu, P.-P. Kung, M. Pairish, L. Jia, J. Meng, L. Funk, I. Botrous, M. McTigue, N. Grodsky, K. Ryan, E. Padrique, G. Alton, S. Timofeevski, S. Yamazaki, Q. Li, H. Zou, J. Christensen, B. Mroczkowski, S. Bender, R. S. Kania and M. P. Edwards, *J. Med. Chem.*, 2011, **54**, 6342–6363; (b) R. Singh, E. S. Masuda and D. G. Payan, *J. Med. Chem.*, 2012, **55**, 3614–3643; (c) J. Felding, M. D. Sørensen, T. D. Poulsen, J. Larsen, C. Andersson, P. Refer, K. Engell, L. G. Ladefoged, T. Thormann, A. M. Vinggaard, P. Hegardt, A. Søhøj and S. F. Nielsen, *J. Med. Chem.*, 2014, **57**, 5893–5903; (d) T. W. Johnson, P. F. Richardson, S. Bailey, A. Brooun, B. J. Burke, M. R. Collins, J. J. Cui, J. G. Deal, Y.-L. Deng, D. Dinh, L. D. Engstrom, M. He, J. Hoffman, R. L. Hoffman, Q. Huang, R. S. Kania, J. C. Kath, H. Lam, J. L. Lam, P. T. Le, L. Lingardo, W. Liu, M. McTigue, C. L. Palmer, N. W. Sach, T. Smeal, G. L. Smith, A. E. Stewart, S. Timofeevski, H. Zhu, J. Zhu, H. Y. Zou and M. P. Edwards, *J. Med. Chem.*, 2014, **57**, 4720–4744; (e) J. Popovici-Muller, R. M. Lemieux, E. Artin, J. O. Saunders, F. G. Salituro, J. Travins, G. Cianchetta, Z. Cai, D. Zhou, D. Cui, P. Chen, K. Straley, E. Tobin, F. Wang, M. D. David, V. Penard-Lacronique, C. Quivoron, V. Saada, S. Botton, S. Gross, L. Dang, H. Yang, L. Utley, Y. Chen, H. Kim, S. Jin, Z. Gu, G. Yao, Z. Luo, X. Lv, C. Fang, L. Yan, A. Olaharski, L. Silvermann, S. Biller, S.-S. M. Su and K. Yen, *ACS Med. Chem. Lett.*, 2018, **9**, 300–305; (f) D. L. Grand, M. Gosling, U. Baettig, P. Bahra, K. Bala, C. Brocklehurst, E. Budd, R. Butler, A. K. Cheung, H. Choudhury, S. P. Collingwood, B. Cox, H. Danahay, L. Edwards, B. Everatt, U. Glaenzel, A.-L. Glotin, P. Groot-Kormelink, E. Hall, J. Hatto, C. Howsham, G. Hughes, A. King, J. Koehler, S. Kulkarni, M. Lightfoot, I. Nicholls, C. Page, G. Pergl-Wilson, M. O. Popa, R. Robinson, D. Rowlands, T. Sharp, M. Spendiff, E. Stanley, O. Steward, R. J. Taylor, P. Tranter, T. Wagner, H. Watson, G. Williams, P. Wright, A. Young and D. A. Sandham, *J. Med. Chem.*, 2021, **64**, 7241–7260.
- For selected reviews, see: (a) D. M. Stout and A. I. Meyers, *Chem. Rev.*, 1982, **82**, 223–243; (b) U. Eisner and J. Kuthan, *Chem. Rev.*, 1972, **72**, 1–42; (c) M. C. Bagley, C. Glover and E. A. Merritt, *Synlett*, 2007, 2459–2482.
- For selected reviews, see: (a) B. Heller and M. Hapke, *Chem. Soc. Rev.*, 2007, **36**, 1085–1094; (b) J. A. Varela and C. Saá, *Chem. Rev.*, 2003, **103**, 3787–3802.
- For selected reviews, see: (a) J. M. Neely and T. Rovis, *Org. Chem. Front.*, 2014, **1**, 1010–1015; (b) M. Behforouz and M. Ahmadian, *Tetrahedron*, 2000, **56**, 5259–5288; (c) A. V. Gulevich, A. S. Dudnik, N. Chernyak and V. Gevorgyan, *Chem. Rev.*, 2013, **113**, 3084–3213.
- For selected examples, see: (a) K. Parthasarathy, M. Jeganmohan and C.-H. Cheng, *Org. Lett.*, 2008, **10**, 325–328; (b) P. C. Too, T. Noji, Y. J. Lim, X. Li and S. Chiba, *Synlett*, 2011, 2789–2794; (c) T. K. Hyster and T. Rovis, *Chem. Commun.*, 2011, **47**, 11846–11848; (d) D. A. Colby, R. G. Bergman and J. A. Ellman, *J. Am. Chem. Soc.*, 2008, **130**, 3645–3651; (e) J. M. Neely and T. Rovis, *J. Am. Chem. Soc.*, 2013, **135**, 66–69; (f) J. M. Neely and T. Rovis, *J. Am. Chem. Soc.*, 2014, **136**, 2735–2738.
- For reviews on Umpolung reactivity, see: (a) X. Bugaut and F. Glorius, *Chem. Soc. Rev.*, 2012, **41**, 3511–3522; (b) D. Seebach, *Angew. Chem. Int. Ed. Engl.*, 1979, **18**, 239–258; (c) B.-T. Gröbel and D. Seebach, *Synthesis*, 1977, 357–402.
- For selected examples of the α -cation-stabilizing effect of *O*-alkyl oximes, see: (a) X. Creary, Y.-X. Wang and Z. Jiang, *J. Am. Chem. Soc.*, 1995, **117**, 3044–3053; (b) X. Creary and Z. Jiang, *J. Org. Chem.*, 1996, **61**, 3482–3489; (c) X. Creary, E. A. Burtch and Z. Jiang, *J. Org. Chem.*, 2003, **68**, 1117–1127; (d) M. Schlegel and C. Schneider, *Org. Lett.*, 2018, **20**, 3119–3123; (e) M. Schlegel and C. Schneider, *Chem.*



Commun., 2018, **54**, 11124–11127; (f) R. Narayan, R. Fröhlich and E.-U. Würthwein, *J. Org. Chem.*, 2012, **77**, 1868–1879.

9 Reviews for Umpolung of carbonyl groups by hydrazone formation, see: (a) R. Lazny and A. Nodzewska, *Chem. Rev.*, 2010, **110**, 1386–1434; (b) R. Brehme, D. Enders, R. Fernandez and J. M. Lassaletta, *Eur. J. Org. Chem.*, 2007, 5629–5660; for selected examples of the electrophilic addition at β -position of α,β -unsaturated hydrazones, see: (c) T. Hashimoto, H. Kimura and K. Maruoka, *Angew. Chem., Int. Ed.*, 2010, **49**, 6844–6847.

10 For selected examples of Umpolung reactivity of α,β -unsaturated oximes, see: (a) Y. Hashimoto, H. Ishiwata, S. Tachikawa, S. Ban, N. Morita and O. Tamura, *Chem. Commun.*, 2017, **53**, 2685–2688; (b) M. Furugori, K. Yoshida, Y. Hashimoto, N. Morita and O. Tamura, *Chem. Pharm. Bull.*, 2021, **69**, 1010–1016; (c) N. Umemoto, A. Imayoshi and K. Tsubaki, *Tetrahedron Lett.*, 2020, **61**, 152213–152216. For examples of the electrophilic addition at β -position of α,β -unsaturated oximes, see: (d) A. M. Chibiryakov, A. Y. Denisov, D. V. Pyshnyi and A. V. Tkachev, *Russ. Chem. Bull.*, 2001, **50**, 1410–1418; (e) R. Fernandes, K. Mhaske, R. Balhara, G. Jindal and R. Narayan, *Chem.-Asian J.*, 2022, **17**, e202101369.

11 T. Yamada, Y. Hashimoto, K. Tanaka III, N. Morita and O. Tamura, *J. Org. Chem.*, 2020, **85**, 12315–12328.

12 T. Yamada, Y. Hashimoto, K. Tanaka III, N. Morita and O. Tamura, *Org. Lett.*, 2021, **23**, 1659–1663.

13 (a) X. Fu, J. Yang, K. Deng, L. Shao, C. Xia and Y. Ji, *Org. Lett.*, 2019, **21**, 3505–3509; (b) X.-P. Fu, S.-B. Tang, J.-Y. Yang, L.-L. Zhang, C.-C. Xia and Y.-F. Ji, *Eur. J. Org. Chem.*, 2019, 5974–5977.

14 J. He, S. Li, Y. Deng, H. Fu, B. N. Laforteza, J. E. Spangler, A. Homs and J.-Q. Yu, *Science*, 2014, **343**, 1216–1220.

15 (a) C. Jia, D. Piao, J. Oyamada, W. Lu, T. Kitamura and Y. Fujiwara, *Science*, 2000, **287**, 1992–1995; (b) W. Lu, Y. Yamaoka, Y. Taniguchi, T. Kitamura, K. Takaki and Y. Fujiwara, *J. Organomet. Chem.*, 1999, **580**, 290–294; (c) C. Jia, W. Lu, J. Oyamada, T. Kitamura, K. Matusda, M. Irie and Y. Fujiwara, *J. Am. Chem. Soc.*, 2000, **122**, 7252–7263; (d) P. K. Hota, A. Jose and S. K. Mandal, *Organometallics*, 2017, **36**, 4422–4431.

16 CCDC-2166741 (**18**) contains the ESI † crystallographic data for this paper.

17 (a) Computations were carried out with the Gaussian 09 series of programs. M. J. Frisch, *et al.*, *Gaussian 09, Revision D.01*, Gaussian Inc., Wallingford, CT, 2013, see complete reference in the ESI † . All compounds were calculated with ω B97X-D/6-311+G(d,p), and an ultrafine grid was used for geometry optimization; (b) J.-D. Chai and M. Head-Gordon, *Phys. Chem. Chem. Phys.*, 2008, **10**, 6615–6620.

18 Structures have been represented in the figures using CLYview. C. Y. Legault, *CYLview, 1.0b*, Université de Sherbrooke, 2009, <https://www.cylview.org>.

19 For selected examples, see: (a) S. I. Gorelsky, D. Lapointe and K. Fagnou, *J. Am. Chem. Soc.*, 2008, **130**, 10848–10849; (b) D. Garcia-Cuadrado, P. de Mendoza, A. A. C. Braga, F. Maseras and A. M. Echavaren, *J. Am. Chem. Soc.*, 2007, **129**, 6880–6886; (c) M. Lafrance, C. N. Rowley, T. K. Woo and K. Gagnou, *J. Am. Chem. Soc.*, 2006, **128**, 8754–8756; (d) D. Lapointe and K. Fagnou, *Chem. Lett.*, 2010, **39**, 1118–1126; (e) D. L. Davies, S. M. A. Donald and S. A. Macgregor, *J. Am. Chem. Soc.*, 2005, **127**, 13754–13755; (f) S. I. Gorelsky, D. Lapointe and K. Fagnou, *J. Org. Chem.*, 2012, **77**, 658–668.

20 In the presence of water, hydrolysis of the oximes proceeded preferentially. Therefore, it could not be applied to water.

21 For selected examples, see: N. Kanekiyo, T. Kuwada, T. Choshi, J. Nobuhiro and S. Hibino, *J. Org. Chem.*, 2001, **66**, 8793–8798. (b) B. M. Trost and A. C. Gutierrez, *Org. Lett.*, 2007, **9**, 1473–1476; (c) S. Liu and L. S. Liebeskind, *J. Am. Chem. Soc.*, 2008, **130**, 6918–6919; (d) K. Tanaka, H. Mori, M. Yamamoto and S. Katsumura, *J. Org. Chem.*, 2001, **66**, 3099–3110.

